

PRODUCTION OF Nb₃Sn FILM ON COPPER SUBSTRATE BY THE BRONZE ROUTE AND THE RF CHARACTERIZATION OF SAMPLES WITH THE QUADRUPOLE RESONATOR

M. Lu^{1,2,*}, S. Keckert¹, F. Kramer¹, A. Zubtsovskii³, A. Prudnikava¹, J. Knobloch^{1,3}, O. Kugeler¹

¹Helmholtz-Zentrum Berlin für Materialien und Energie GmbH, Berlin, Germany

²Institute of Modern Physics, Chinese Academy of Sciences, Lanzhou, China

³Universität Siegen, Siegen, Germany

Abstract

Copper-based Nb₃Sn cavity is a promising candidate for next generation accelerator applications in the field of superconducting radio frequency (SRF). It combines the excellent thermal conductivity of copper and the superior superconducting properties of Nb₃Sn, and has the potential to greatly improve the performance of the SRF cavity. The electrochemical and thermal synthesis (ETS) bronze route is one of the proven methods to achieve Nb₃Sn coating on copper. Its advantages are low cost, simple operation, suitable for complex cavity types and mass production. In this report, we have prepared a copper-based Nb₃Sn sample specifically for Quadrupole Resonator (QPR) testing. We provide a complete set of QPR sample preparation processes from copper electropolishing, Nb sputtering, electrodeposition and heat treatment to synthesize Nb₃Sn. By optimizing the entire preparation process and key parameters, a new Cu-based Nb₃Sn QPR sample was successfully prepared and its RF properties have been characterized by QPR testing system at HZB.

INTRODUCTION

Nb₃Sn has emerged as a promising alternative for next generation superconducting radio-frequency (SRF) cavities, offering a higher critical temperature ($T_c \sim 18$ K) and significantly lower BCS surface resistance (R_s), thereby enabling efficient operation at elevated temperatures such as 4.2 K while maintaining high quality factors (Q_0) [1, 2]. The most mature Nb₃Sn coating technique for SRF cavities is the tin vapor diffusion (TVD) method [3, 4], in which tin vapor reacts with a bulk Nb cavity surface at ~ 1100 °C to form A15 Nb₃Sn layer. However, this approach fundamentally requires Nb as the substrate and is not applicable to low-melting-point materials, such as copper (melting point: 1085 °C).

Copper offers several intrinsic advantages as an SRF cavity substrate, including superior thermal conductivity, lower material cost, and excellent formability [5]. To enable the use of Cu substrates, several alternative Nb₃Sn film deposition methods have been investigated, including magnetron sputtering [6, 7], chemical vapor deposition (CVD) [8], and adaptations of the classical bronze process [9, 10]. Among these, the bronze route stands out as a viable and scalable method for synthesizing Nb₃Sn films on Cu surfaces.

Traditionally developed for multifilamentary Nb₃Sn wire fabrication [11, 12], the bronze route involves solid-state diffusion between Nb and a Cu–Sn alloy at elevated temperatures, forming the superconducting A15 phase within a Cu matrix. Recent work by Barzi *et al.* has adapted this principle to thin-film applications through a modified electrochemical–thermal synthesis (ETS) process [13]. In this method, a high-purity Nb substrate can be replaced by a Cu substrate coated with a Nb diffusion barrier, followed by the electrochemical deposition of a bronze (Cu–Sn) precursor layer. Subsequent vacuum annealing at intermediate temperatures (typically 700 °C) promotes interdiffusion and reaction to form a uniform Nb₃Sn layer on the surface [14]. Finally, the residual bronze layer on the surface can be removed by chemical etching, thereby exposing a clean Nb₃Sn surface suitable for subsequent RF characterization. [14].

In this study, we report the fabrication and RF characterization of the Cu-based Nb₃Sn sample prepared via the bronze route for application in superconducting cavities. The sample was evaluated using the Quadrupole Resonator (QPR) at Helmholtz-Zentrum Berlin (HZB) to determine its surface resistance [15]. Measurements of the surface resistance (R_s) were performed as functions of both peak magnetic field and temperature, primarily at a frequency of 412 MHz. This allowed for detailed assessment of how R_s varies under different RF field and temperature. In addition, thermal cycling experiments were conducted by cooling the samples at various rates to study the impact of different cooldown procedures on R_s , providing insights into the effects of thermal history and flux trapping on superconducting performance. The critical temperature (T_c) of the Nb₃Sn films was also determined from the temperature-dependent resonant frequency measurements. In addition, the T_c was obtained from magnetization measurements using a Physical Property Measurement System (PPMS) and the surface quality was visually inspected using photographic images. Together, these tests contributed to evaluating the film quality and provided guidance for its further improvement.

EXPERIMENTAL SETUP AND METHODS

The Cu-based Nb₃Sn QPR sample was fabricated through a multi-step bronze route process, as summarized in Fig. 1. The Cu substrate underwent mechanical polishing followed by electrochemical polishing (EP) using a disk-and-belt cathode setup at 2.1 V and 15 °C for one hour, which removed

* email: ming.lu@helmholtz-berlin.de

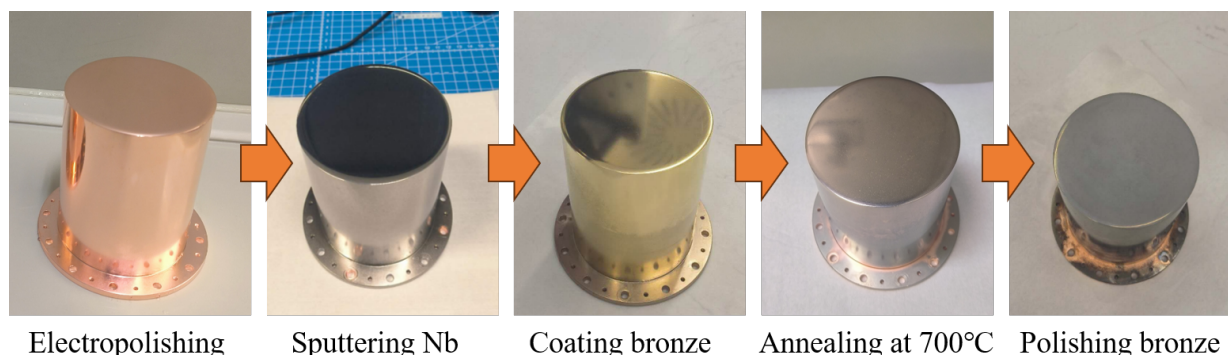


Figure 1: Process flowchart of the Cu-based Nb₃Sn QPR sample preparation via the bronze route, including Cu electropolishing, Nb barrier deposition, bronze electroplating, vacuum annealing, post-polishing.

about 30 μm of copper and reduced average surface roughness below 1 μm .

A 10 μm -thick Nb diffusion barrier was then deposited by high-power impulse magnetron sputtering (HiPIMS) at 180 $^{\circ}\text{C}$. Next, 700 $^{\circ}\text{C}$ annealing was applied to relieve thermal stress caused by the mismatched thermal expansion coefficients of Nb and Cu, thereby minimizing the risk of film cracking. Subsequently, a bronze layer of approximately 10 μm was electroplated onto the Nb-coated Cu substrate. The plating was performed with the sample oriented upside-down to minimize the risk of copper particle sedimentation from the anode and to reduce impurity incorporation, using carefully controlled parameters: 0.3 A current, 15 $^{\circ}\text{C}$ bath temperature, 100 rpm stirring speed, and a deposition time of 2 hours. These parameters were derived from combined simulation and experimental optimization to ensure uniform tin content and consistent thickness of the bronze precursor layer.

Thermal diffusion annealing to form the superconducting Nb₃Sn A15 phase was carried out in high vacuum through a two-step process: 600 $^{\circ}\text{C}$ for 30 hours to initiate interdiffusion, then 700 $^{\circ}\text{C}$ for another 30 hours to complete the phase formation. Heating and cooling rates were strictly maintained at 0.5 $^{\circ}\text{C}/\text{min}$ and 9 $^{\circ}\text{C}/\text{min}$, respectively, to minimize stress and cracking. The vacuum was kept below 5×10^{-9} mbar at room temperature and 6×10^{-8} mbar at 700 $^{\circ}\text{C}$ to prevent oxidation.

After annealing, the surface was chemically etched in two steps. The first step employed a mixed acid solution of H₃PO₄ (85 wt%) and HNO₃ (65 wt%) for 30 minutes to remove residual bronze. The second step involved a 30-minute polishing in an aqueous solution of HF (48 wt%), H₂SO₄ (96 wt%), and deionized H₂O to remove niobium oxides. Subsequently, ultrasonic cleaning followed by high-pressure deionized water rinsing was carried out in a cleanroom environment to remove residual surface contaminants. This procedure ensured the exposure of a clean Nb₃Sn surface, which is critical for achieving high RF performance.

The bronze route provides a thermodynamically stable and compositionally adjustable approach for fabricating high-quality Nb₃Sn films on Cu substrates. However, achieving

uniform and low surface resistance (R_s) Nb₃Sn films on Cu via the bronze route remains a major challenge [16]. In particular, precise control over Sn diffusion and interfacial reactions at the Nb/Nb₃Sn boundary is essential to ensure phase purity and RF-grade microstructure. Moreover, critical issues such as internal stress arising from thermal expansion mismatch, Cu inclusions, Sn-rich secondary phases, and oxide contamination persist and severely degrade the superconducting and RF performance.

RESULTS AND DISCUSSION

A thorough evaluation of the RF properties is crucial for assessing the feasibility of Cu-based Nb₃Sn films in practical SRF cavity applications. The Quadrupole Resonator (QPR), a widely adopted and highly precise tool, enables detailed characterization of the RF surface resistance (R_s) and superconducting performance [17, 18]. In this work, the Cu-based Nb₃Sn sample was systematically examined through comprehensive QPR measurements, thermal cycling tests, and surface morphology analyses. The results reveal key challenges, including stoichiometric non-uniformity, surface contamination, Cu inclusions, and the need for optimized thermal treatment parameters. Nevertheless, the findings also demonstrate the promising potential of the bronze route for synthesizing high-quality Nb₃Sn thin films on copper substrates.

Surface Resistance and Thermal Cycling

Figure 2 shows the R_s of the Nb₃Sn/Cu sample measured at 412 MHz as a function of peak magnetic field at various temperatures. At 2 K and 5 mT, R_s reached 76 n Ω , which is substantially higher than the 33 n Ω observed for a reference Nb/Cu sample at 15 mT [19]. The strong field dependence (Q-slope) indicates the presence of non-ideal mechanisms such as residual resistance, weak links at grain boundaries, and impurity scattering.

The influence of thermal cycling on surface resistance is shown in the left panel of Fig. 3. The sample was subjected to different cooling rates between 10 K and 2 K. In contrast to the behavior typically observed in Nb₃Sn films,

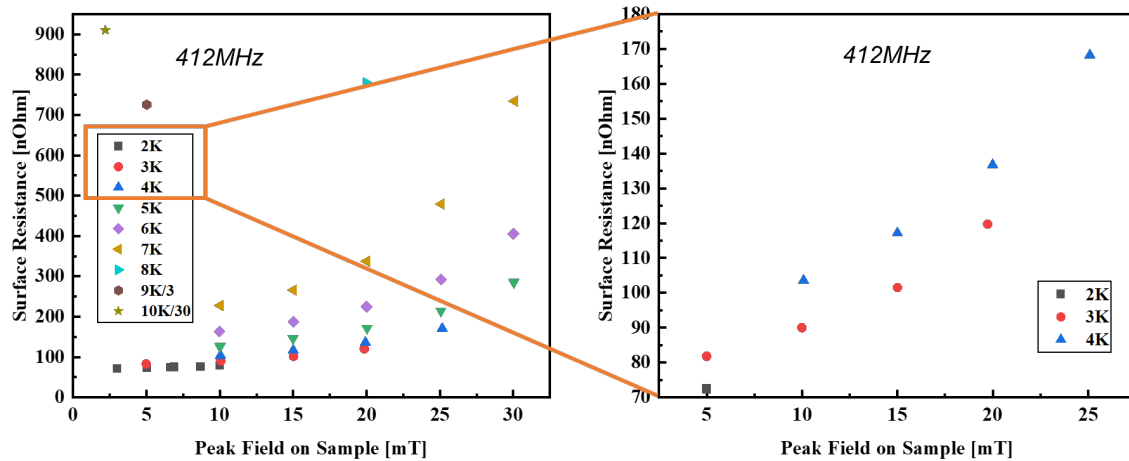


Figure 2: Surface resistance R_s vs. peak magnetic field at 412 MHz and different temperatures for the Cu-based Nb_3Sn sample. A strong Q-slope is observed at low temperature.

the difference in R_s between faster and slower cooldowns was negligible, even at low field. This suggests that the film exhibits strong flux pinning, likely arising from a high density of defects and spatial variations in Sn stoichiometry, which suppress the sensitivity of the residual resistance to cooldown dynamics. Such behavior implies that trapped flux is already saturated regardless of the applied thermal gradient.

In the right panel of Fig. 3, the R_s vs. field behavior at 824 MHz is presented. At $B_p = 5$ mT, the measured R_s is about 227 n Ω at 2.5 K, indicating excessive RF losses. Although R_s generally increases with frequency as expected from BCS theory, the magnitude and nonlinearity at 824 MHz are more pronounced compared to 412 MHz. This suggests that at higher frequency, additional loss channels—such as surface oxides, residual tin-rich phases, or normal-conducting grain boundary regions—become more significant due to their higher RF dissipation. However, because the number of available data points in this measurement is limited, no further quantitative analysis was performed.

Superconducting Transition and Stoichiometry

Figure 4 presents the superconducting transition temperature (T_c) characterization of the Nb_3Sn films. The left panel shows the T_c extracted from the Quadrupole Resonator (QPR) frequency versus temperature measurement, yielding a value of 14.5 K. The right panel displays the magnetization-temperature (M–T) curve measured by a Physical Property Measurement System (PPMS) on a small sample prepared using the same process, with an extracted T_c of 14.4 K. The close agreement between these two independent measurements confirms the reliability of the results. Compared to pure Nb, which exhibits a sharp transition at 9.2 K, the broader transition and reduced T_c of Nb_3Sn can be attributed

to stress induced by lattice mismatch, an inhomogeneous Sn distribution, and Sn loss due to the porous structure of the Nb_3Sn layer, leading to local Sn-deficient and Sn-rich regions as well as overall compositional and microstructural inhomogeneities that degrade the superconducting properties.

Surface Morphology and Process Optimization for Cu-Based Nb_3Sn Films

After annealing and chemically etching, the Nb_3Sn surface exhibits distinct dark regions and localized exposure of the underlying Cu substrate, as also shown in Fig. 5. These features are attributed to incomplete coverage or porosity in the Nb barrier layer. The porous areas likely facilitated Cu diffusion into the Nb_3Sn film during thermal treatment, resulting in contamination, local phase decomposition, and degradation of superconducting properties. Such defective regions exhibit high electrical resistance and disproportionately increase the RF surface resistance (R_s), especially under high-field or high-frequency conditions.

To address these issues, improvements are necessary at multiple stages. Enhancing the Cu substrate quality by optimizing electrochemical polishing (EP) parameters can significantly reduce surface defects and pore formation. Increasing the density and thickness of the sputtered Nb barrier, or alternatively introducing a thin Ta interlayer, can improve barrier integrity and reduce porosity. Furthermore, optimizing the thermal treatment profile is essential to control the Sn content and grain size of Nb_3Sn , thereby minimizing flux pinning centers. Lastly, refining the chemical etching recipe and duration after annealing will help eliminate surface oxides and secondary phases without damaging the Nb_3Sn layer, thereby minimizing surface contamination and improving superconducting performance.

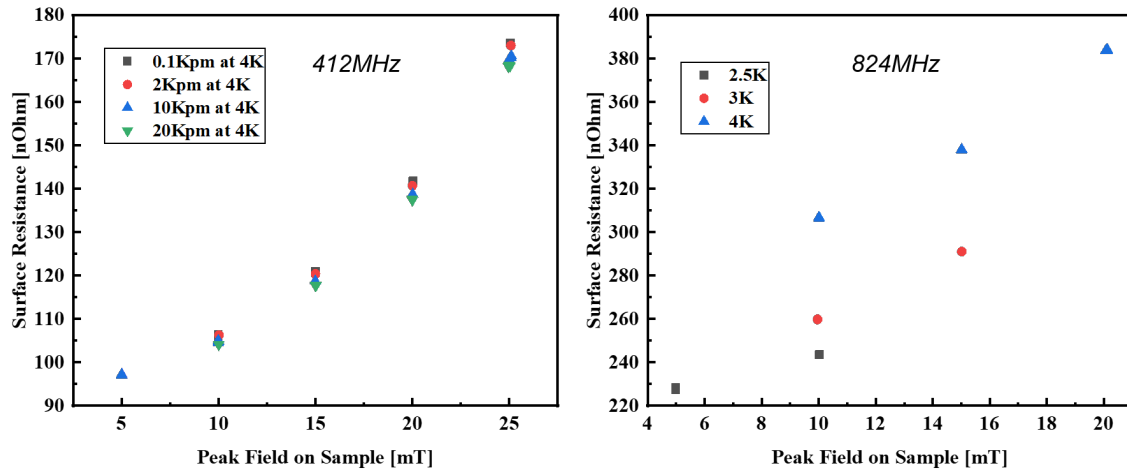


Figure 3: Left: Surface resistance R_s at 412 MHz under different thermal cycling procedures. Right: R_s vs. peak magnetic field at 824 MHz showing increased losses and stronger nonlinearity at higher frequency.

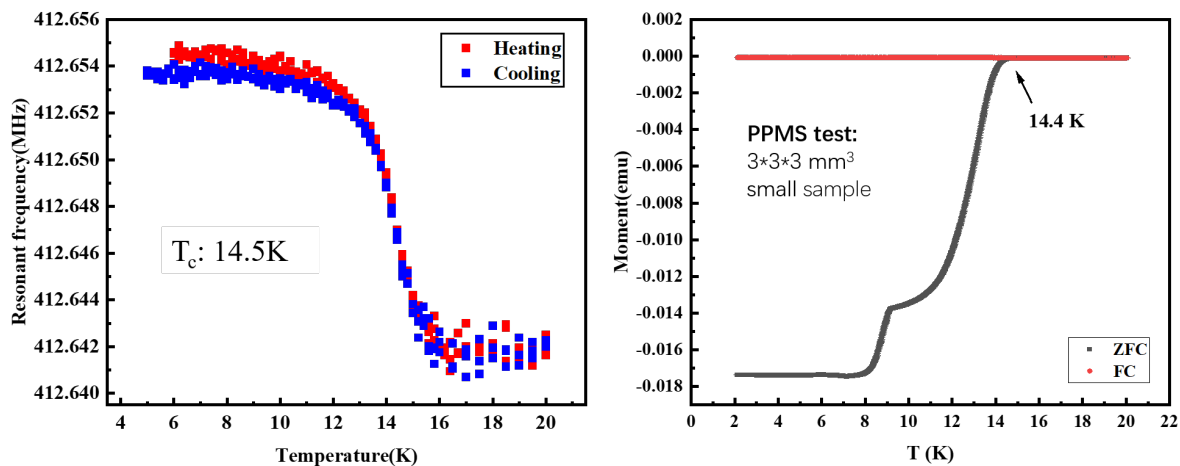


Figure 4: Superconducting transition temperature (T_c) of the Nb_3Sn film. Left: $T_c = 14.5$ K from QPR frequency–temperature measurement. Right: $T_c = 14.4$ K from M–T curve of a companion sample.

CONCLUSIONS

This study demonstrates the feasibility of fabricating Cu-based Nb_3Sn films via the bronze route and evaluating their superconducting radio-frequency (SRF) performance using a quadrupole resonator (QPR). The sample exhibited superconducting behavior with a surface resistance of 76 n Ω at 2 K, 5 mT and 412 MHz. However, the RF performance remains limited by several structural and compositional factors, leaving substantial room for improvement.

The superconducting transition was broad (12–16 K), indicating significant spatial inhomogeneity in Sn stoichiometry. Surface inspections revealed submicron defects on the Cu substrate and signs of incomplete barrier coverage. Surface characterization showed localized Cu exposure, oxygen contamination. These issues contributed to increased residual

resistance and pronounced field-dependent losses. Additionally, thermal cycling studies indicated negligible sensitivity to flux trapping, likely due to strong flux pinning arising from a high density of lattice defects and microstructural inhomogeneity in the film.

To enhance film quality and performance, several processing refinements are necessary. Increasing the Sn content in the bronze precursor layer to 15–20 at.% aims to provide sufficient Sn for complete A15 phase formation while avoiding Sn excess that could lead to the formation of Sn-rich secondary phases. Enhancing the density and continuity of the Nb diffusion barrier—e.g., by increasing the Nb deposition temperature above 600 °C using high-temperature HiPIMS—can effectively improve the density of the Nb barrier layer. Moreover, the Nb thickness should be increased

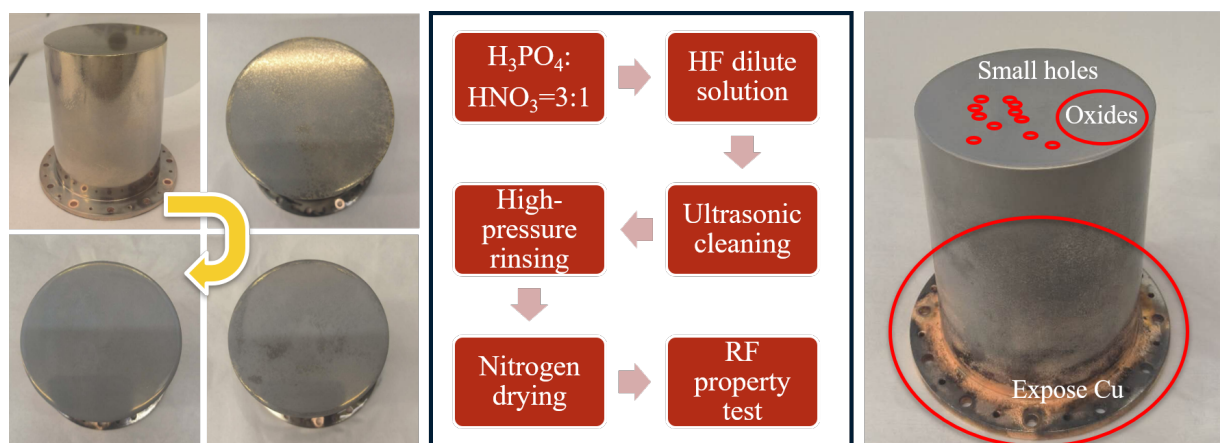


Figure 5: Optical image of the Cu substrate after chemical polishing. Submicron pits and local surface irregularities are still visible, which can initiate non-uniform growth and impurity entrapment.

to at least 30 μm to ensure adequate blocking performance. Further improvements may be achieved by introducing a dense Ta diffusion barrier as an alternative or additional interlayer. Finally, optimization of heat treatment parameters and post Nb_3Sn surface cleaning recipes is essential for reducing oxide residues and mitigating surface defects.

In summary, this work provides a foundational step toward the development of scalable, cost-effective $\text{Nb}_3\text{Sn}/\text{Cu}$ SRF cavities using the bronze route. While further process optimization is required to achieve state-of-the-art performance, the successful synthesis and characterization presented here highlight a promising route for future application in next-generation SRF technologies.

ACKNOWLEDGMENTS

We gratefully acknowledge I. Rudolph for granting access to the chemical facilities at the WI-APG department of HZB. We also thank R. Feyerherm from the QM-IQM department at HZB for performing the PPMS measurements. This work has received partial funding from the European Union's Horizon 2020 Research and Innovation programme under Grant Agreement No. 101004730 (LFAST). Additional support was provided by the German Federal Ministry of Education and Research (BMBF) under Grant No. 100636506 (Cavity-SusOp, within the SuperSurfer framework).

REFERENCES

- [1] C. Becker *et al.*, "Analysis of Nb_3Sn surface layers for superconducting radio frequency cavity applications", *Appl. Phys. Lett.*, vol. 106, no. 8, p. 082602, 2015. doi:10.1063/1.4913617
- [2] A. Godeke, "A review of the properties of Nb_3Sn and their variation with A15 composition, morphology and strain state", *Supercond. Sci. Technol.*, vol. 19, no. 8, p. R68, 2006. doi:10.1088/0953-2048/19/8/R02
- [3] G. Jiang *et al.*, "Understanding and optimization of the coating process of the radio-frequency Nb_3Sn thin film superconducting cavities using tin vapor diffusion method", *Appl. Surf. Sci.*, vol. 643, p. 158708, 2024. doi:10.1016/j.apsusc.2023.158708
- [4] S. Posen, M. Liepe, and D. Hall, "Proof-of-principle demonstration of Nb_3Sn superconducting radiofrequency cavities for high Q_0 applications", *Appl. Phys. Lett.*, vol. 106, no. 8, p. 082601, 2015. doi:10.1063/1.4913247
- [5] E. Barzi *et al.*, "An Impartial Perspective for Superconducting Nb_3Sn coated Copper RF Cavities for Future Accelerators", 2022. doi:10.48550/arXiv.2203.09718
- [6] M. N. Sayeed, U. Pudasaini, C. E. Reece, G. V. Ereemeev, and H. E. Elsayed-Ali, "Properties of Nb_3Sn films fabricated by magnetron sputtering from a single target", *Appl. Surf. Sci.*, vol. 541, p. 148528, 2021. doi:10.1016/j.apsusc.2020.148528
- [7] E. A. Ilyina *et al.*, "Development of sputtered Nb_3Sn films on copper substrates for superconducting radiofrequency applications", *Supercond. Sci. Technol.*, vol. 32, no. 3, p. 035002, 2019. doi:10.1088/1361-6668/aaf61f
- [8] G. Carta, G. Rossetto, P. Zanella, L. Crociani, V. Palmieri, and F. Todescato, "Attempts to Deposit Nb_3Sn by MOCVD", in *Proc. 9th Int. Conf. on Thin Films for Supercond. RF Appl. (TFSRF 2006)*, Padua, Italy, 2006.
- [9] W. K. Withanage, A. Juliao, and L. D. Cooley, "Rapid Nb_3Sn film growth by sputtering Nb on hot bronze", *Supercond. Sci. Technol.*, vol. 34, no. 6, p. 06LT01, 2021. doi:10.1088/1361-6668/abf66f
- [10] M. Lu *et al.*, "Electrochemical and thermal synthesis of Nb_3Sn coatings on Nb substrates", *Mater. Lett.*, vol. 292, p. 129557, 2021. doi:10.1016/j.matlet.2021.129557
- [11] C. Sanabria, M. Field, P. J. Lee, H. Miao, J. Parrell, and D. C. Larbalestier, "Controlling Cu-Sn mixing so as to enable higher critical current densities in RRP® Nb_3Sn wires", *Supercond. Sci. Technol.*, vol. 31, no. 6, p. 064001, 2018. doi:10.1088/1361-6668/aab8dd
- [12] T. Laurila, V. Vuorinen, A. Kumar, and A. Paul, "Diffusion and growth mechanism of Nb_3Sn superconductor grown by bronze technique", *Appl. Phys. Lett.*, vol. 96, no. 23, p. 231910, 2010. doi:10.1063/1.3453502

- [13] E. Barzi, M. Bestetti, F. Reginato, D. Turrioni, and S. Franz, “Synthesis of superconducting Nb₃Sn coatings on Nb substrates”, *Supercond. Sci. Technol.*, vol. 29, no. 1, p. 015 009, 2015. doi:10.1088/0953-2048/29/1/015009
- [14] E. Barzi and S. Mattafirri, “Kinetics of phase growth in Nb₃Sn formation for heat treatment optimization”, Fermilab, Batavia, IL, USA, Rep. FERMLAB-Conf-02/176-E, 2002.
- [15] S. Keckert, R. Kleindienst, O. Kugeler, D. Tikhonov, and J. Knobloch, “Characterizing materials for superconducting radiofrequency applications—A comprehensive overview of the quadrupole resonator design and measurement capabilities”, *Rev. Sci. Instrum.*, vol. 92, no. 6, p. 064 710, 2021. doi:10.1063/5.0046971
- [16] M. Lu *et al.*, “Development and Performance of the First Nb₃Sn Thin-Film Cavity via Bronze Process”, *Chin. Phys. Lett.*, vol. 39, no. 11, p. 115 201, 2022. doi:10.1088/0256-307X/39/11/115201
- [17] S. Bira, M. Ge, A.-M. Valente-Feliciano, L. V. Cid, and W. V. Delsolaro, “Geometry Optimization for a Quadrupole Resonator at Jefferson Lab”, in *Proc. SRF’23*, Grand Rapids, MI, USA, pp. 670–673, 2023. doi:10.18429/JACoW-SRF2023-WEPWB048
- [18] Y. Zhao, S. Huang, M. Yu, L. Peng, and Y. He, “RF design for a quadrupole resonator with a fundamental frequency of 325 MHz at IMP”, *J. Phys.: Conf. Ser.*, vol. 3094, no. 1, p. 012 048, 2025. doi:10.1088/1742-6596/3094/1/012048
- [19] M. Lu *et al.*, “Preparation of the First Cu-based Nb₃Sn Sample via Bronze Route for Quadrupole Resonator Testing”, 2025. doi:10.48550/arXiv.2509.11224